Sergii BESPALKO[1], Jerzy MIZERACZYK[2]
Research and Innovation Centre Pro-Akademia (1), Gdynia Maritime University, Department of Marine Electronics (2)
ORCID: 1. https://orcid.org/0000-0002-7542-5498; 2. https://orcid.org/0000-0002-5173-3592

doi:10.15199/48.2023.09.54

Influence of the ballast resistor on the current-voltage characteristics in the cathodic subregimes of the plasma-driven solution electrolysis

Streszczenie. *W artykule przedstawiono wyniki badań eksperymentalnych charakterystyk prądowo-napięciowych w elektrolizie stałoprądowej 10-procentowego roztworu wodnego Na_2CO_3 obejmujących trzy reżimy operacyjne: Faradyczny, przejściowy oraz reżim elektrolizy roztworu napędzanego plazmą (PDSE). Podano interpretację charakterystyki prądowo-napięciowej, szczególnie dla reżimu elektrolizy PDSE, który składa się z dwóch podrejonów: stabilnych i gwałtownych wyładowań jarzeniowych. Badanie to po raz pierwszy pokazuje wpływ rezystora balastowego wprowadzonego szeregowo do obwodu ogniwa elektrolitycznego na prąd i napięcie robocze, a także pobór mocy do podtrzymania wyładowań jarzeniowych. Tak więc, wprowadzenie rezystancji balastowej 15 Ohm zmniejsza pobór mocy do podtrzymania wyładowań jarzeniowych o 44%. Diagnostyka optycznej spektroskopii emisyjnej (OES) pokazuje sekwencję pojawiania się linii emisyjnych Na, OH i Hα, gdy reżim przejściowy i podreżimy katodowego PDSE są osiągane wraz ze wzrostem przyłożonego napięcia stałego. (**Wpływ rezystora balastowego na charakterystykę prądowo-napięciową w podregionach katodowych elektrolizy roztworu napędzanego plazmą**)*

Abstract. *The paper presents the results of an experimental study of the current-voltage characteristics in the DC electrolysis of 10 wt% Na_2CO_3 aqueous solution covering three operational regimes: Faradaic, transition, and regime of the plasma-driven solution electrolysis (PDSE). An interpretation of the current-voltage characteristic is given, especially for the PDSE regime of electrolysis, which is composed of two subregimes: stable and violent glow discharges. This study shows for the first time an influence of the ballast resistor introduced in series to the electrolytic cell circuit on the operating current and voltage as well as power consumption to sustain the glow discharges. Thus, introducing the ballast resistance of 15 Ohm decreases power consumption needed to sustain the glow discharges by 44%. The optical emission spectroscopy diagnostics (OES) shows a sequence of the appearance of the Na, OH, and H_α emission lines when the transition regime and subregimes of the cathodic PDSE are attained with an increase of the applied DC voltage.*

Słowa kluczowe: Elektroliza, elektroliza plazmowa roztworów, wyładowania elektryczne w cieczach, wodór, charakterystyka prądowo-napięciowa, rezystor balastowy.
Keywords: Electrolysis, plasma-driven solution electrolysis, electric discharges in liquids, hydrogen, current-voltage characteristic, ballast resistor.

Introduction

Currently, there is a great interest in various electrochemical methods of hydrogen production [1]. One of the reasons is that hydrogen is considered an essential element of the future energy supply chain based on intermittent renewable electricity [2].

Recently, some attention was given to hydrogen production in the plasma-driven solution electrolysis (PDSE), also called plasma electrolysis or contact glow discharge electrolysis. This is due to the high values of the Faradaic yield of hydrogen achieved in the experiments, which are several to dozens of times higher than the theoretical limit of the Faradaic electrolysis [3, 4].

There is a number of published papers explaining the current-voltage characteristics and transformation of the electrolysis from its Faradaic regime to the PDSE regime, which can be found in our review paper [5]. However, in some papers [6, 7], the use of the ballast resistor in the electrical circuit of the cell is mentioned, while other papers [8, 9] do not contain any details on it.

The lack of information regarding the role of the ballast resistor in attaining the plasma formation at the discharge electrode inspired us to conduct the current study. Thus, the current study aims to determine the influence of the ballast resistor introduced in series to the electrolytic cell circuit on the current-voltage characteristics of the DC electrolysis covering Faradaic, transition, and PDSE regimes.

Experimental setup and procedure

Fig. 1a shows a schematic of the experimental setup used to study the current-voltage characteristics of the DC electrolysis of 10 wt% Na_2CO_3 aqueous solution covering the Faradaic, transition, and PDSE regimes. Fig. 1b shows a photo of the electrolytic cell.

a)

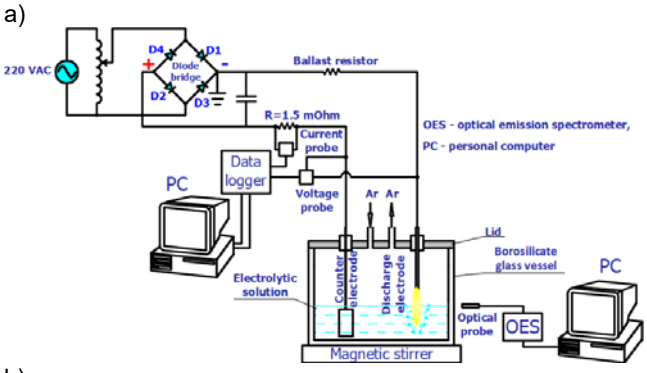

b)

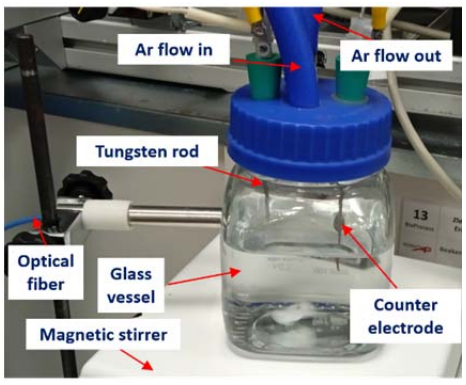

Fig. 1. The experimental setup: a) a scheme of the experimental setup, b) a photo of the electrolytic cell.

The electrolytic solution was 500 grams of 10 wt% Na_2CO_3 aqueous solution. The electrodes: Ni foam plate with 25 mm × 25 mm active surface area exposed to the electrolytic solution (anode) and a tungsten rod with a diameter of 2 mm (cathode). The Ni foam plate was immersed in the electrolytic solution to a depth of 25 mm. The tungsten rod was immersed in the electrolytic solution to a depth of 1.5 mm. The distance between electrodes was 45 mm.

The borosilicate glass vessel was filled with 500 g of 10 wt% Na_2CO_3 aqueous solution and served as the electrolytic cell. The initial temperature of the electrolytic solution was 22 ℃. Two metal electrodes of different shapes and polarities were immersed in the electrolytic solution. The electrode with a larger active surface area of 25 mm × 25 mm, made of Ni foam (Nanografi), being positively charged, served as a counter electrode. While the tungsten rod with a diameter of 2 mm and length of an active surface area of 1.5 mm, being negatively charged, served as the discharge electrode. Since the cathode's active surface area was much smaller than the anode's, the increased applied voltage led to the plasma formation at the cathode. The electrolytic cell was membraneless and served as a batch reactor without exchanging the electrolytic solution. Argon at a flow rate of 1 sLpm was used as a purge gas to evacuate all gas products from the electrolytic cell.

The LTC-300-8D (RUCELF) variable autotransformer of 2.4 kVA nominal power equipped with a diode bridge and two smoothing capacitors of 16 mF (Kemet) served as the DC power supply. A variable ballast resistor was installed in series to the electrolytic cell circuit. It allowed us to set the ballast resistance at 0 Ohm, 2 Ohm, and 15 Ohm.

In the electrochemical cell, the voltage between the cathode and anode was measured by a WAD-A-MAX-608 (Acon) high-voltage probe (-600 V ÷ +600 V), while the current flowing between two electrodes was measured by a voltage drop across a resistor (the electric shunt) of 1.5 mOhm using a precision isolation amplifier WAD-A-MAX-609 (Acon) (-225 mV ÷ +225 mV). A WAD-AD12-128H (Acon) data logger recorded all current and voltage probe signals. The data acquisition frequency was set at 1 Hz for each probe.

Optical emission spectroscopy diagnostics (OES) was carried out on the electric discharges using a UV-Vis-NIR spectrometer LR2 (Lasertack). The light emission spectra from 200 nm to 1200 nm were captured each second of the experiment. The optical probe was installed in the stainless-steel pipe outside the electrochemical cell and placed in front of the discharge electrode tip. Neither a focusing lens nor a pinhole was applied to capture the light emitted from the discharge electrode. The exposure time was set at 10 ms. The spectra were processed using Spectra+ (Lasertack) spectroscopy software.

The current and voltage were recorded simultaneously with increasing applied DC voltage from 0 V to 120 V for 100 seconds. In each measurement of the IV characteristic, the temperature of the electrolytic solution increased due to the Joule heating by app. 2 ℃. The video record and OES also accompanied the increase of the applied voltage. This allowed us to identify the onset time of the plasma formation at the discharge electrode. After acquiring the data, MATLAB 2016b was applied for mathematical data processing and presenting the collected data as graphical and tabular representations.

Results and discussion

The typical form of the current-voltage characteristic

Fig. 2 presents the typical form of the current-voltage characteristic, showing the transformation of DC electrolysis from its Faradaic regime (marked I) through the transition regime (marked II) to the PDSE regime (marked III) of electrolysis at the negatively charged smaller electrode.

In the section “ab”, the electric current rises exponentially when the voltage increases. This regime, typically occurring in alkaline electrolyzers, is called the Faradaic regime of the DC electrolysis.

At point “b”, an inflection of the IV characteristic occurs because the nucleate boiling is initiated at the discharge electrode. Actually, due to the small active surface area of the discharge electrode exposed to the electrolytic solution, at a certain value of the applied voltage, the current density at the discharge electrode reaches the critical value at which the nucleate boiling begins. For this reason, in the section “bc”, two processes occur simultaneously: Faradaic electrolysis and nucleate boiling. This explains the slight rise of the electric current with an increase in the applied voltage.

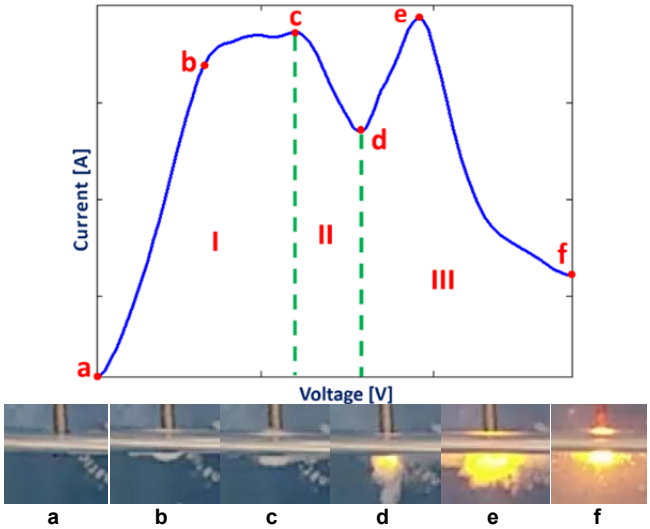

Fig. 2. Typical form of the current-voltage characteristic with the marked specific points and photos of the discharge electrode corresponding to those specific points:
a – the origin of the Faradaic electrolysis, b – the beginning of the bubble nucleation, c – the breakdown point (the first current maximum), d – the discharge onset point, e – the second current maximum, f – the endpoint in the violent glow discharge subregime. Voltage regions: I – the Faradaic regime of electrolysis, II – the transition regime, III – the PDSE regime.

At point “c”, the first current maximum is achieved. In the scientific literature [10], this point is also referred to as the breakdown point, and the applied voltage corresponding to this point is called the breakdown voltage. Further increase of the applied voltage beyond the breakdown point leads to the formation of the transition regime (section “cd”) of the DC electrolysis when the bubbles’ cluster blocks the discharge electrode from the bulk electrolyte. This explains the significant drop in the electric current. However, the electric current is not zero because the electrons participate in the charge transfer through the interfacial region between bubbles in the cluster, and the first electric discharge is initiated.

At point “d”, a stable gas-vapor film is formed around the active surface area of the discharge electrode, and ionization of the gas-vapor film begins. In the scientific literature [10], this point is called the discharge onset point, with the corresponding applied voltage called the discharge onset voltage. Beyond the breakdown point, the PDSE regime of electrolysis occurs.

Further increase of the applied voltage beyond the discharge onset voltage (section “de”) leads to the high ionization of the gas-vapor film resulting in blanketing the discharge electrode with the glow discharges. The plasma supports the charge transfer when the voltage is increased. This explains the rise of the electric current in section “de” with the increase of the applied voltage.

At point “e”, the second current maximum is achieved. The high electric current value achieved at point “e” results

in a significant evaporation rate of the bulk electrolytic solution surrounding the discharge electrode. At this stage, the glow discharge plasma at the electrode becomes larger and bright.

In the section “ef”, an increase of the applied voltage leads to the transformation of the stable glow discharges to the violent glow discharges. At this stage, much heat is released. As a result, the upper part of the tungsten rod becomes hot and red, as seen in Fig. 2 (point “f”). Because of the high evaporation rate of the surrounding electrolytic solution, the overall electric resistance significantly soars up, resulting in a significant drop in the electric current. That is why the IV curve of the section “ef” is falling.

Therefore, the PDSE regime of electrolysis (see region III in Fig. 2) consists of two subregimes. The first subregime (section “de”) is characterized by stable glow discharges at the discharge electrode, and the second subregime (section “ef”) is characterized by violent glow discharges and much heat release.

Influence of the ballast resistor on the current-voltage characteristics

Similarly to the gas discharges, in the current study, we used the ballast resistor of different values installed in series to the electrolytic cell circuit for stabilizing the plasma formation at the discharge electrode.

Fig. 3 shows the current-voltage characteristics measured at different values of the ballast resistance.

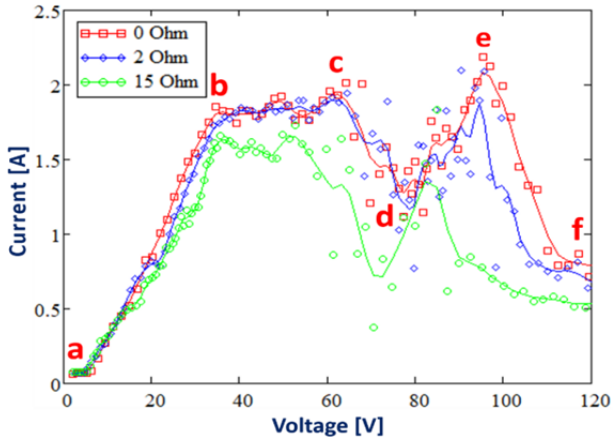

Fig. 3. Current-voltage characteristics of the DC electrolysis of 10 wt% Na_2CO_3 aqueous solution measured using the ballast resistance of 0 Ohm, 2 Ohm, and 15 Ohm covering the Faradaic, transition, and the PDSE regimes.

It is seen from Fig. 3 that the increase of the ballast resistance from 0 to 15 Ohm decreased the values of the electric current and voltage in those characteristic points (i.e., “b”, “c”, “d”, “e”, “f”) on the current-voltage characteristics.

Values of the voltage, current, and power corresponding to point “e” of the current-voltage characteristics presented in Fig. 3 are shown in Table 1.

Table 1. The values of the electric current, voltage, and power corresponding to point “e” (the second current maximum) on the current-voltage characteristics (shown in Fig. 3) in the cathodic PDSE of 10 wt% Na_2CO_3 aqueous solution for various ballast resistors

Resistance, Ohm	Voltage, V	Current, A	Power, W	Photos
0	95.423	2.085	198.957	
2	94.687	1.878	177.822	
15	82.323	1.357	111.712	

As seen from Table 1, introducing the ballast resistor of 15 Ohm decreases in point “e” the voltage by 13.1 V and the electric current by 0.728 A. This leads to a decrease in the power consumption by almost 44%. That is why the plasma region around the discharge electrode is smaller with the ballast resistor than the case without the ballast resistor.

It is worth mentioning that values of the current and voltage corresponding to the points “b”, “c”, “d”, and “e”, as well as a form of the current-voltage characteristic, are extremely sensitive to the diameter and immersion depth of the discharge electrode, the material of the discharge electrode, temperature, and conductivity of the electrolytic solution, type of the electrolytic solution, presence of organic and other additives, etc. This will be elaborated on in our future studies.

The OES results

Fig. 4 shows the light spectra emitted by the electric discharges at the discharge electrode in three sections (“cd”, “de”, and “ef”) of the current-voltage characteristic in the cathodic PDSE with a ballast resistance of 15 Ohm.

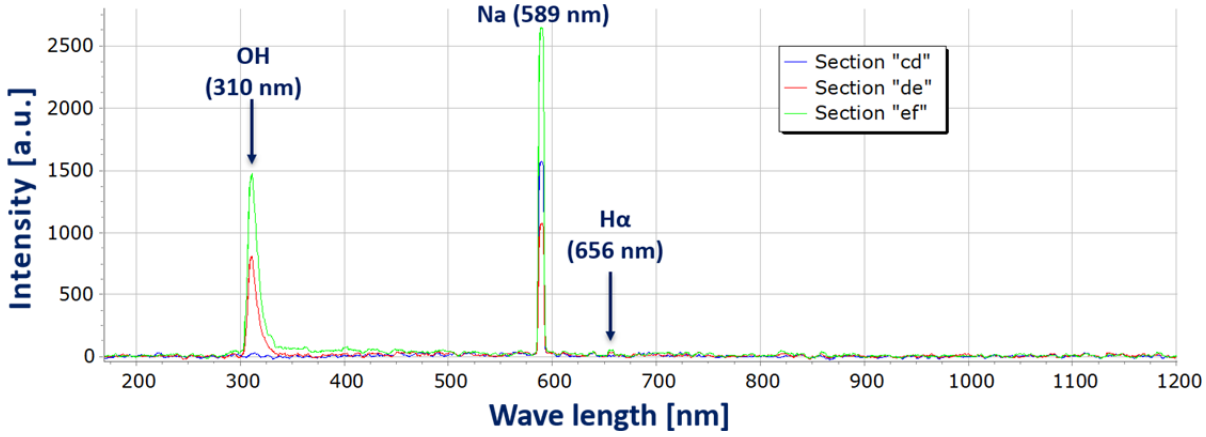

Fig. 4. OES spectra of the light emitted from the electric discharges at the discharge electrode in the three sections “cd”, “de”, and “ef” of the current-voltage characteristic of the cathodic PDSE regime of electrolysis of 10 wt% Na_2CO_3 aqueous solution with the ballast resistor of 15 Ohm. The spectra were captured at the following applied DC voltage and current: blue line at 66.8 V and 0.87 A, red line at 79.8 V and 1.06 A, green line at 102 V and 0.6 A.

In the section “cd”, when the first electric discharge appears at the discharge electrode, only one emission line is observed at 589 nm corresponding to Na (see blue line in Fig. 4) with the emission intensity of about 1600 a.u. Increasing the applied voltage beyond the discharge onset voltage (section “de”) leads to the appearance of the additional emission lines in the UV range with a peak at 310 nm and an intensity of about 1500 a.u. (red line), which corresponds to the emission line of OH radical. This confirms the origin of the water molecules’ decomposition by the electric discharges.

Further increase of the applied DC voltage transforms the stable glow discharges to violent glow discharges. The falling section “ef” of the current-voltage characteristic is attained. In this section, in addition to the emission lines of Na and OH, a small emission peak appears at 656 nm, corresponding to H_α line (green line).

Conclusions

Summing up the results of this experimental study, the following conclusions can be drawn:

An increase in the applied voltage between two electrodes immersed in the electrolytic solution leads to the sequential transformation of the DC electrolysis from its Faradaic regime through the transition regime to the PDSE regime. The current-voltage characteristic of this transformation contains the following sections: “ab” – Faradaic electrolysis, “bc” – Faradaic electrolysis combined with boiling, “cd” – transition regime when the stable gas-vapor film is formed around the discharge electrode, “de” – ionization of the gas-vapor film (stable glow discharge subregime of the cathodic PDSE), “ef” – the transformation of the stable glow discharges to the violent glow discharges characterized by the strong heating effect (violent glow discharge subregime of the cathodic PDSE).

Introducing the ballast resistor positively influences the decrease of power consumption needed to sustain the glow discharges at the discharge electrode. Thus, using the ballast resistance of 15 Ohm leads to decreased voltage and electric current, resulting in a drop in power consumption needed to sustain the plasma in point “e” by 44%. This can essentially increase the energy efficiency of hydrogen production in the PDSE regime of electrolysis.

For the first time, a sequence of the appearance of the Na, OH, and Hα emission lines is shown when the violent subregime of PDSE is attained with an increase of the applied DC voltage.

Sergii Bespalko would like to thank the Polish National Agency for Academic Exchange (NAWA) for the funding under the Ulam Program – Seal of Excellence (the grant agreement no. PPN/SEL/2020/1/00004/U/00001).

Authors: *dr.ing. Sergii Bespalko, Research and Innovation Centre Pro-Akademia, Innowacyjna Street 9/11, 95-050 Konstantynów Łódzki, E-mail: sergii.bespalko@proakademia.eu. prof. dr hab. ing. Jerzy Mizeraczyk, Gdynia Maritime University, Department of Marine Electronics, Morska Street 81/87, 81-225 Gdynia, E- mail: j.mizeraczyk@we.umg.edu.pl*

REFERENCES

[1] Lamb, J.J., Hillestad, M., Rytter, E., Bock, R., Nordgård, A.S., Lien, K.M., Burheim, O.S., & Pollet, B.G. Chapter 3 - Traditional Routes for Hydrogen Production and Carbon Conversion; Jacob J. Lamb, Bruno G. Pollet, Eds.; In Hydrogen and Fuel Cells Primers, Hydrogen, Biomass and Bioenergy, Academic Press, (2020) pp. 21-53, https://doi.org/10.1016/B978-0-08-102629-8.00003-7

[2] Peterssen, F., Schlemminger, M., Lohr, C., Niepelt, R., Bensmann, A., Hanke-Rauschenbach, R., & Brendel, R. Hydrogen supply scenarios for a climate neutral energy system in Germany. *International Journal of Hydrogen Energy*. 47 (28) (2022), 13515-13523 https://doi.org/10.1016/j.ijhydene.2022.02.098

[3] Yan, Z.C.; Li, C.; Lin, W.H. Hydrogen generation by glow discharge plasma electrolysis of methanol solutions. *Int. J. Hydrogen Energy*, *34 (*2009), 48–55. https://doi.org/10.1016/j.ijhydene.2008.09.099

[4] Toth, J.R.; Hawtof, R.; Matthiesen, D.; Renner, J.; Sankaran, R.M. On the non-faradaic hydrogen gas evolution from electrolytic reactions at the interface of a cathodic atmospheric-pressure microplasma and liquid water surface. *J. Electrochem. Soc.*, *167 (*2020), 116504. https://doi.org/10.1149/1945-7111/aba15c

[5] Bespalko, S.; Mizeraczyk, J. Overview of the Hydrogen Production by Plasma-Driven Solution Electrolysis. *Energies*, *15 (*2022*)*, 7508. https://doi.org/10.3390/en15207508

[6] Hickling, A. Electrochemical Processes in Glow Discharge at the Gas-Solution Interface. In: Bockris, J.O., Conway, B.E. (eds) Modern Aspects of Electrochemistry No. 6 (1971) Springer, Boston, MA. https://doi.org/10.1007/978-1-4684-3000-4_5

[7] Kravchenko, A., Berlizova, S.A., Nesterenko, A.F., & Kublanovskii, V.S. On the Change in Properties of Water Subjected to Low-Temperature Plasma Electrolysis. *High Energy Chemistry, 38* (2004), 333-337. https://doi.org/10.1023/B%3AHIEC.0000041345.07168.FD

[8] Saksono, N., Harianingsih, Farawan, B., Luvita, V., & Zakaria, Z. Reaction pathway of nitrate and ammonia formation in the plasma electrolysis process with nitrogen and oxygen gas injection. *Journal of Applied Electrochemistry*, (2023), 1-9. https://doi.org/10.1007/s10800-023-01849-4

[9] Alteri, G., Bonomo, M., Decker, F., & Dini, D. Contact Glow Discharge Electrolysis: Effect of Electrolyte Conductivity on Discharge Voltage. *Catalysts*. 10, (2020), 1104. https://doi.org/10.3390/CATAL10101104

[10] Susanta K Sen Gupta and Rajshree Singh *Plasma Sources Sci. Technol.* 26 (2017), 015005 https://doi.org/10.1088/0963-0252%2F26%2F1%2F015005